

# CONSIDERATION OF A NON-HYDROSTATIC ATMOSPHERE-OCEAN COUPLED MODEL FOR SIMULATING TROPICAL CYCLONES

Tomoki Shirai<sup>1</sup> and Taro Arikawa<sup>2</sup>

Accurate prediction of coastal hazards, such as tropical cyclones (TC), storm surges, and high waves, is essential for mitigating damage and saving lives. While TC track prediction accuracy has significantly improved, the prediction of TC intensity variables, like minimum central pressure and maximum wind speed, has seen limited progress. A critical factor in enhancing TC intensity prediction is the consideration of the interactions between TCs and the ocean, particularly ocean cooling caused by vertical mixing and upwelling. Recent advancements in computational capacity have enabled the use of three-dimensional (3D) ocean models, overcoming the limitations of simpler models such as slab or one-dimensional mixed layer models. Recently, some studies have shown that non-hydrostatic solvers can influence ocean responses to TCs in the open ocean. In this study, we aim to develop a model that can consistently predict phenomena of various scales, from ocean response to TCs in the open ocean to coastal inundation during TCs by using the STOC (Storm Surge and Tsunami Simulator in Oceans and Coastal Areas, Tomita and Kakinuma 2005), which was originally developed for simulating storm surges, as a 3D model. In this paper, as a first step, the potential and challenges of using the STOC model for non-hydrostatic ocean simulations will be explored through preliminary atmosphere-ocean coupling simulation results.

*Keywords: WRF; STOC; non-hydrostatic coupled modeling*

## Tropical Cyclone (TC) Prediction and TC-Ocean Interactions

Accurate prediction of coastal hazards due to tropical cyclones (TC), such as storm surges and high waves, which lead to coastal flooding, is a crucial task for saving lives. Today, TC prediction is fundamentally based on numerical simulations. Prediction uncertainties are significant due to multiple factors such as initial conditions, physical processes, and model computation settings. On the other hand, by utilizing this prediction information and understanding the situation days before TC landfall helps prepare for these hazards in advance.

The accuracy of TC track predictions has steadily improved (Yu et al., 2022). This improvement owes much to advances in model physics, enhanced grid resolution due to improved computational capacity, and enriched observations coupled with data assimilation (Landsea and Cangialosi, 2018). On the other hand, the accuracy of TC intensity predictions, such as minimum central pressure and maximum wind speed, has lagged behind track improvements (Zhang et al., 2014). One key factor in improving TC intensity prediction is considering TC-ocean interactions. A well-known phenomenon influencing TC intensity is the coupling process between TCs and upper ocean temperature (e.g., Price et al., 1981). Under high SST conditions, the latent heat supply from the ocean increases with stronger winds, intensifying the TC. However, as wind speeds increase, the mixed layer deepens, and cold water from below is brought up, cooling the upper ocean and reducing the heat flux from the ocean (Jacob and Shay, 2003). These effects interact and affect TC intensity. Additionally, vertical advection (upwelling) brings cold water to the surface, and while the effect is smaller, horizontal advection also cools the upper ocean (Zhang et al., 2016). Therefore, considering these effects in models is known to be crucial for improving TC intensity prediction accuracy. For example, Ito et al. (2015) conducted simulations on many TCs using a coupled model that accounted for TC-ocean interactions and reported that incorporating ocean processes improved intensity prediction accuracy by about 20%, reducing the model's bias to overestimate TC intensity.

Several methods exist for incorporating TC-ocean interactions in numerical simulations. Directly solving a 3D ocean model is computationally expensive, so slab models (0D) that approximate the average behavior of the mixed layer are still chosen for global simulations (Zarzycki, 2016). One-dimensional mixed layer models that incorporate vertical turbulent diffusion to homogenize temperature and salinity are also used (Li et al., 2020). Recently, however, with improved computational power, 3D ocean models are increasingly being employed, overcoming the limitations of simpler models. By using 3D models, processes such as Ekman upwelling can be represented, enabling a more realistic simulation of upper ocean responses and interactions with TCs.

---

<sup>1</sup> Civil, Human and Environmental Engineering Course of Graduate School of Science and Engineering, Chuo University, 1-13-27 Kasuga, Bunkyo-ku, Tokyo, 112-8551, Japan (corresponding author)

<sup>2</sup> Department of Civil and Environmental Engineering, Chuo University, 1-13-27 Kasuga, Bunkyo-ku, Tokyo, 112-8551, Japan

Models such as COAWST (Warner et al., 2010), an open-source coupled atmosphere-ocean-wave model, have facilitated many studies on TC-ocean interactions using 3D ocean models (Zhao and Chan, 2016; Li et al., 2022). One of the remaining challenges is accounting for non-hydrostatic processes, which has become more feasible with advancements in computational capacity. Li and Chen (2022) investigated how the choice between hydrostatic and non-hydrostatic solvers in the ocean model FVCOM influences the ocean's response to TCs. Although their model, with a horizontal resolution of 200 m, could not fully capture coastal non-hydrostatic processes, their test case showed that the non-hydrostatic solver strengthened coastal upwelling and intensified sea surface cooling, resulting in a slight reduction (a few hPa) in TC intensity.

Moreover, Aiki et al. (2015) discovered that strong local winds driven by TCs excited internal soliton waves through Ekman upwelling, generating significant vertical velocity signals around 1000 m depth. This was further amplified by the dispersive nature of non-hydrostatic solvers, forming internal soliton wave trains. While non-hydrostatic solvers could alter the ocean's response to TCs and feedback into TC intensity, this effect is not fully understood and requires further validation.

Using non-hydrostatic solvers requires solving a Poisson equation to obtain dynamic pressure under the incompressibility assumption, a computationally expensive task. Models such as CROCO (Marchesiello et al., 2021) avoid solving the Poisson equation by accounting for seawater compressibility. On the other hand, thanks to recent advancements in computational efficiency, major ocean models used as components in air-sea coupled models now frequently implement non-hydrostatic solvers (Garcia et al. 2019 provides a concise review of non-hydrostatic models). Although few studies have utilized non-hydrostatic solvers for TC prediction beyond those mentioned above, exploring how ocean responses change when non-hydrostatic solvers are applied in TC simulations could provide new insights. Such studies would be valuable for optimizing future resource allocation in TC prediction research. However, improving computational efficiency remains an obstacle to conducting such research. Therefore, this study aims to develop a new atmosphere-ocean coupled model using the Storm Surge and Tsunami Simulator in Oceans and Coastal Areas (STOC, Tomita and Kakinuma 2005), a solver developed in the field of coastal engineering that efficiently considers non-hydrostatic effects through nesting functionalities. Here, STOC's applicability and challenges will be examined, and preliminary results from atmosphere-ocean coupling simulations will be introduced.

### Overview of a Coupled Model

For the ocean model, we use STOC, which includes both a hydrostatic solver (STOC-ML, hereafter ML) and a non-hydrostatic solver (STOC-IC, hereafter IC). The basic equations of STOC are based on the following 3D incompressible Reynolds Averaged Navier Stokes Equations (only the equation in the  $x$ -direction is shown):

$$\gamma_v \frac{\partial u}{\partial t} + \frac{\partial}{\partial x} (\gamma_x uu) + \frac{\partial}{\partial y} (\gamma_y uv) + \frac{\partial}{\partial z} (\gamma_z uw) - \gamma_v f_0 v = -\gamma_v \frac{1}{\rho} \frac{\partial p}{\partial x} + F \quad (1)$$

where  $u, v, w$  is velocity components of  $x, y, z$  directions,  $\gamma_x, \gamma_y, \gamma_z$  are transmissivity rates in each direction,  $\gamma_v$  is an effective volume rate which is a rate of volume of liquid in a grid,  $\rho$  is a density of water,  $p$  is a pressure,  $f_0$  is a Coriolis parameter, and the term  $F$  indicates external forces, including the surface drag by winds, the bottom friction, and the viscosity. In STOC-ML, vertical momentum conservation is not solved directly, and vertical velocity is determined to satisfy the continuity equation. STOC defines a single free surface at any arbitrary  $(x, y)$  point using the following equation:

$$\gamma_z \frac{\partial \eta}{\partial t} + \frac{\partial}{\partial x} \int_{-H}^{\eta} \gamma_x u dz + \frac{\partial}{\partial y} \int_{-H}^{\eta} \gamma_y v dz = 0 \quad (2)$$

where  $\eta$  is the deviation of the water level from the still water level, and  $H$  is the water depth. In addition to these basic equations, STOC solves the advection-diffusion equations for scalar quantities such as salinity and temperature. Since convection cannot be explicitly represented in ML, convective adjustment parameterization is implemented. When the stratification condition is not met (i.e., when the lower layer has a lower density), the temperature and salinity are averaged over the layers, including the upper layer, to immediately resolve the unstable state. These basic equations are discretized using the finite volume method based on control volumes on a staggered grid, with time integration performed using the leapfrog method. In IC, the Poisson equation is solved using the MILU-BiCGStab method. Since STOC allows IC and ML to be connected through nesting, regions of interest can be solved with IC while other areas are solved with ML, enabling efficient computations.

Both IC and ML support domain decomposition and parallel computing using the Message Passing Interface (MPI).

For the atmospheric model, we use the Weather Research and Forecasting model (WRF) (Skamarock et al., 2008), which is based on the fully compressible 3D non-hydrostatic Euler equations. WRF includes physics options to represent subgrid-scale phenomena such as cloud microphysics and atmospheric boundary layers. WRF serves as the atmospheric model within the COAWST system, coupled with the ocean model (ROMS) and the wave model (SWAN) through the MCT coupler. In this study, we adopt the coupler as one of the coupling methods. At the time of writing, debugging of the coupling method using the coupler is still ongoing by the authors, but we plan to introduce the STOC model as a new ocean component in the COAWST system. The advantages of this method include incorporating STOC with minimal modifications to the coupler and associated subroutines, facilitating future coupling with SWAN, and allowing each model to be consistently controlled by the COAWST master program, which executes the subroutines and exchanges input/output data from each component without file I/O, improving efficiency. Another implemented coupling method simply controls both models with an execution script, exchanging restart file data between WRF and STOC using a Python script based on the model output results (this mode is called “restart run mode”). Although this method is slightly less efficient due to file I/O, interpolation, and restart process, it is physically equivalent to the coupler-based method that exchanges variables between models every few hundred seconds.

Although STOC has a proven track record in tsunami and storm surge simulations, its applicability as an ocean model for atmosphere-ocean coupled simulations aimed at TC prediction has not been well studied. In the next section, we will test whether STOC can be used as an ocean model before conducting WRF-STOC coupled simulations.

#### Applicability of STOC as an Ocean Model

As an initial test, we confirmed STOC’s capability to simulate surface ocean cooling in response to TC forcing. Below are the conditions for the test calculations. First, we confirmed that TC response simulations, including scalars, could be stably conducted in both ML and IC under a fixed typhoon case (not shown). Next, STOC was driven using real TC forcing from Typhoon Faxai (T1915). According to Iida et al. (2023), as Faxai passed, a maximum sea surface temperature (SST) decreases of up to 2 °C, biased to the right side of its track, was observed. STOC was run without considering tides, assuming a uniform depth (1000 m) and an idealized topography, with the f-plane approximation (25°N). The domain coverage of the STOC is 117.0-162.0°E, 3.0-48.0°N. The simulation was run for 78 hours, starting at 18:00 UTC on 5 September, 2019. The simulation started from a calm state, and mean sea level pressure and 10 m wind speed from WRF were provided hourly. The WRF run was forced 6 hourly by the NCEP FNL (Final) analysis (d083003), and physics options were selected based on Shirai et al. (2022) (WSM5 for the cloud microphysics, MYJ for the planetary boundary layer, and other schemes were same as Shirai et al.). For this initial test, we simplified the problem by ignoring surface scalars (e.g., radiation, precipitation). The vertical distributions of temperature and salinity were assumed uniform horizontally, with the values derived from the spatial average of CMEMS data over the same horizontal domain as STOC for a specific time during Faxai. The vertical distribution is

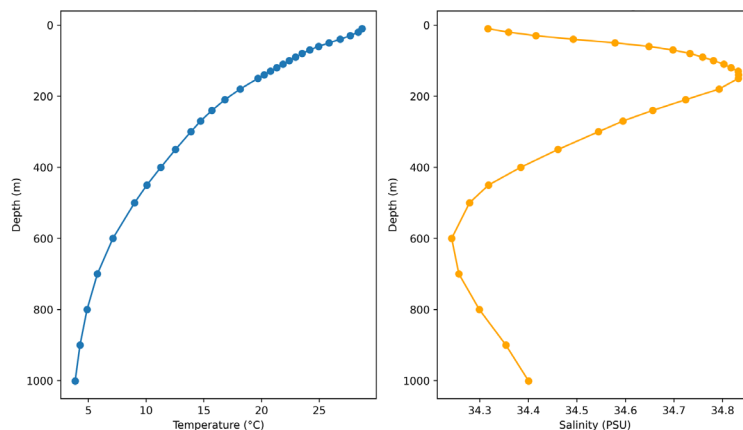


Figure 1. Initial vertical distribution of the scalar variables (left) temperature, (right) salinity.

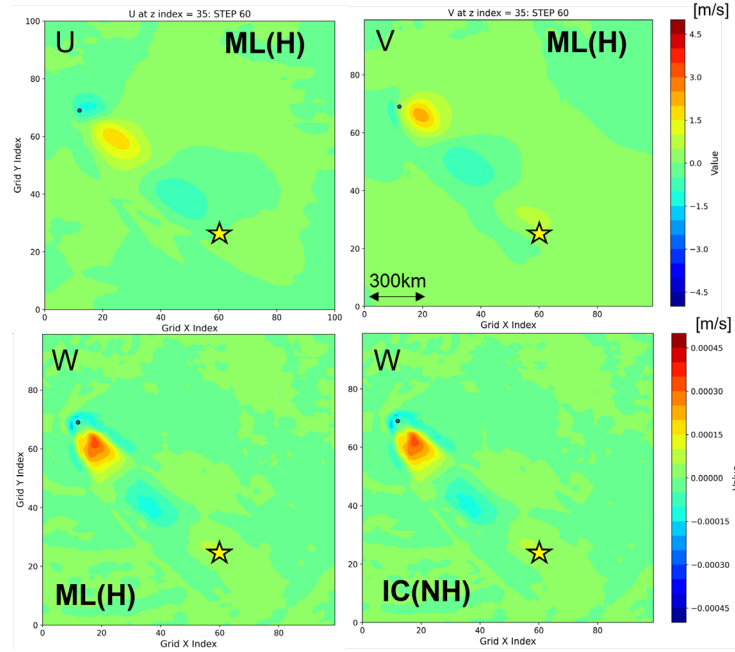


Figure 2. Snapshots of velocity components at the surface. The blue dot indicates the TC center.

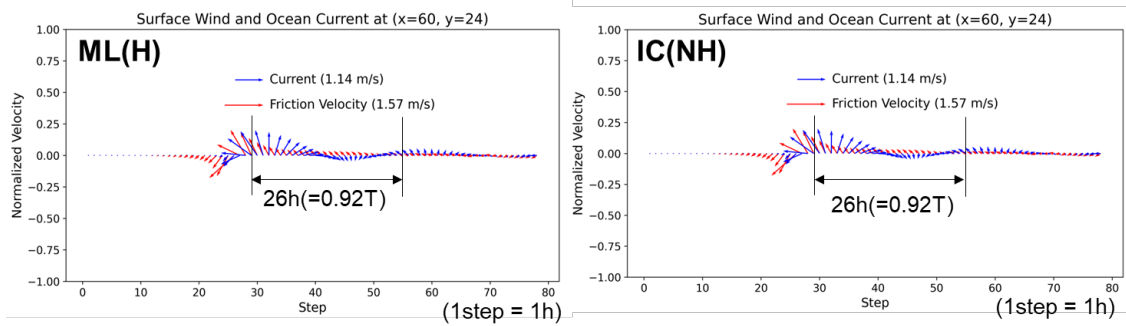


Figure 3. Time series of the ocean surface current and friction velocity at the specific point.

shown in Figure 1. The horizontal resolution of both WRF and STOC was 15 km for this test, and STOC had 36 vertical levels. The vertical grid was coarser in deeper regions and finer in shallower regions, with resolutions ranging from 100 m to 10 m. Although STOC incorporates turbulence models like a TKE (turbulence kinetic energy)-based one, it was not possible to introduce them under the current conditions due to simulation instability. This instability might have arisen from the use of free boundary conditions. Similar issues could have occurred with temperature and salinity, but the simulations were stabilized by expanding the simulation domain to mitigate TC-induced variability at the boundaries, thereby roughly satisfying the zero-gradient assumption at the boundary. As a future work, it may be effective to use 3D ocean GPV data like CMEMS for lateral boundary values and implement nudging boundaries in STOC.

Next, we present the results. Figure 2 shows snapshots of current velocity from both ML and IC ( $w$  only). The vertical upward motions occurred behind the TC, with an order of magnitude of  $\sim O(10^{-4})$ , that are consistent with previous studies (e.g., Price et al.). The maximum horizontal velocity was about 3 m/s, and little difference was observed between ML and IC results. This is likely due to (1) the surface ocean response to the TC being describable on a hydrostatic scale in this case, and (2) the resolution of IC being too coarse to capture non-hydrostatic effects. Figure 3 shows the time series of surface ocean current vectors and friction velocity vectors from the wind at the yellow star point in Figure 2. A southwesterly velocity component appeared just before the TC's arrival (around 24 h), and the current direction rotated clockwise, with a period of 26 h, in response to changes in wind direction due to the TC's movement. The inertial period at  $25^\circ$  N is 28.3 h, indicating that this current response is near-inertial oscillation. This oscillation exhibited similar characteristics in both ML and IC under

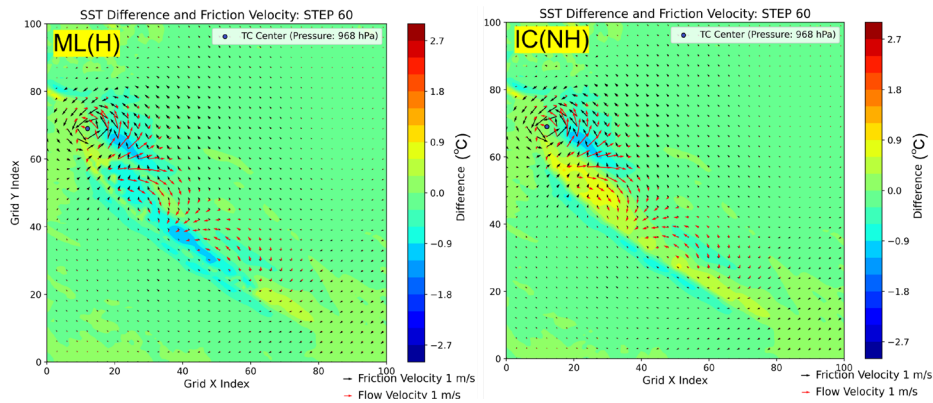


Figure 4. Snapshots of SST deviation (shaded), friction velocity, and surface current.

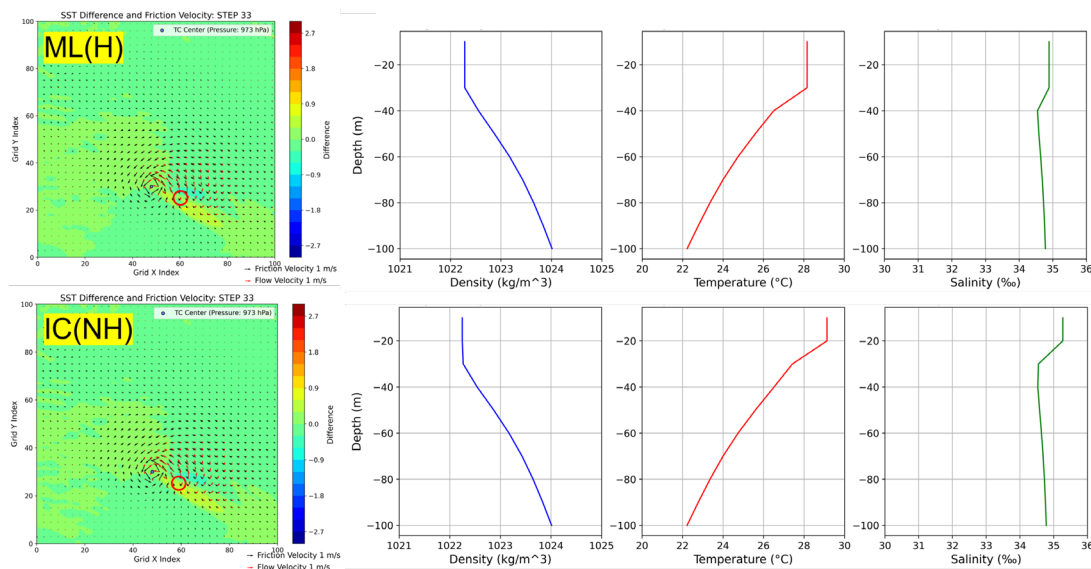


Figure 5. Snapshots of scalar distributions at the red point (upper: ML, bottom: IC).

the conditions of this calculation. It is generally known that the ocean’s surface response to TC passage includes near-inertial oscillations (e.g., Zhang et al., 2021), and this result suggests that STOC can reproduce the surface ocean response to TC passage, at least in terms of current velocity.

Figure 4 shows the temperature anomaly distribution of the uppermost STOC cell (which we refer to as SST for convenience in this study) overlaid with wind and current fields. As seen in the ML results, a decrease in SST is observed along the TC track. The SST decreased by up to about 2 °C over time, which is comparable to the values shown by Iida et al., demonstrating that despite the simplicity of the test conditions, STOC successfully captures the key qualitative and quantitative features of the SST response to the TC. However, in IC, while the typical SST cooling on the right side of the TC was captured similarly to ML, an anomalous SST increase of about +1 °C was observed behind the TC, which is not a general trend. This phenomenon can be partially understood by examining the vertical temperature distribution. Figure 5 shows the calculated vertical profiles of density, temperature, and salinity from the ocean surface to a depth of 100 m behind the TC. The density distribution is similar between ML and IC, but there is a significant difference in the temperature profiles: ML has a deeper isothermal layer, and while the IC isothermal layer exceeds 29 °C, ML is about 1 °C cooler at around 28 °C and is lower than the initial SST of 28.7 °C. This vertical scalar distribution in ML stabilizes after an instantaneous adjustment, likely due to the convective adjustment function implemented in ML. Since IC lacks the convective adjustment used in ML and its coarse resolution fails to resolve vertical convection, there was no provision of cold water from the lower layer, resulting in an apparent SST increase behind the TC. In this paper, high-resolution simulations and ML-IC nested runs have not yet been sufficiently verified to capture the differences between hydrostatic and non-hydrostatic solvers due to computational stability issues within the STOC model. Computational divergence near domain

boundaries requires revising boundary conditions and improving numerical solution methods. Additionally, incorporating turbulence models for stable vertical mixing and upper ocean temperature reduction will be necessary in future work. As mentioned above, several challenges have been identified regarding the use of STOC as an ocean model, such as the need for improvements or adjustments to computational conditions. Nevertheless, the test results clearly demonstrate that ML can reproduce surface ocean cooling to some extent under TC forcing, suggesting that coupled model tests are feasible. In the next section, we will present preliminary results from the first WRF-STOC coupled simulation and discuss future challenges and directions.

### Preliminary Result of the WRF-STOC Coupled Simulation and Future Directions

In this section, we conducted calculations to evaluate the impact of TC using the WRF and STOC coupling executed through the “restart run mode” mentioned in the second section. First, WRF is initialized under a horizontally uniform SST condition. This is achieved by directly rewriting the lower boundary value of WRF (`wrf_lowinp`). The data exchange interval between WRF and STOC was set to 1 hour. The results are shown in Figure 6. In the coupled simulation, WRF considers the SST cooling computed by STOC through the lower boundary value (by updating WRF’s restart file). In contrast, the reference case only includes WRF, so no SST change is reflected. As observed in the previous section, the coupled simulation demonstrated sea surface cooling behind the TC center, which led to a modest central pressure increase of 1-2 hPa. Since the simulation uses idealized oceanic conditions with a coarse resolution, limiting the representation of TC internal structure, quantitative validation against observations remains challenging. Nevertheless, the results indicate that the model successfully captures SST cooling and its associated TC intensity suppression processes. These findings suggest that the WRF-STOC coupled model warrants further development through specific refinements. In particular, the following model enhancements are proposed. (i) Advancing the extension of STOC as an ocean model and improving its computational stability. This includes stabilizing calculations using turbulence models and downscaling computations with oceanic GPV data as lateral boundary values. Additionally, addressing issues where IC calculations become unstable near the boundaries during high-resolution simulations and the instability occurring at the connection boundaries when multilayer IC-ML nesting is applied. (ii) Validating the constructed model. This includes conducting additional sensitivity experiments under idealized conditions, running simulations with realistic topography (not included in this study), and comparing the accuracy with other coupled models.

Thus, while it is true that several computational challenges remain in extending STOC, originally developed as a storm surge and tsunami simulator, as an ocean model, there are still merits in continuing its development for this purpose. First, STOC’s unique strength lies in its ability to integrate hydrostatic and non-hydrostatic solvers, a feature absent in traditional ocean models. Leveraging its H-NH nesting capability, STOC can provide new insights into the role of non-hydrostatic solvers in TC and coastal hazard prediction, a research area gaining increasing attention in ocean modeling. From a longer-term perspective, STOC also holds the potential to connect detailed offshore responses to TCs, including non-hydrostatic processes, with coastal hazards like, storm surges, and inundation events. Additionally, CADMAS-SURF/3D, which adopts the VOF method, allows for solving complex free surfaces including wave breaking, can also be connected to STOC via nesting (Arikawa et al., 2019).

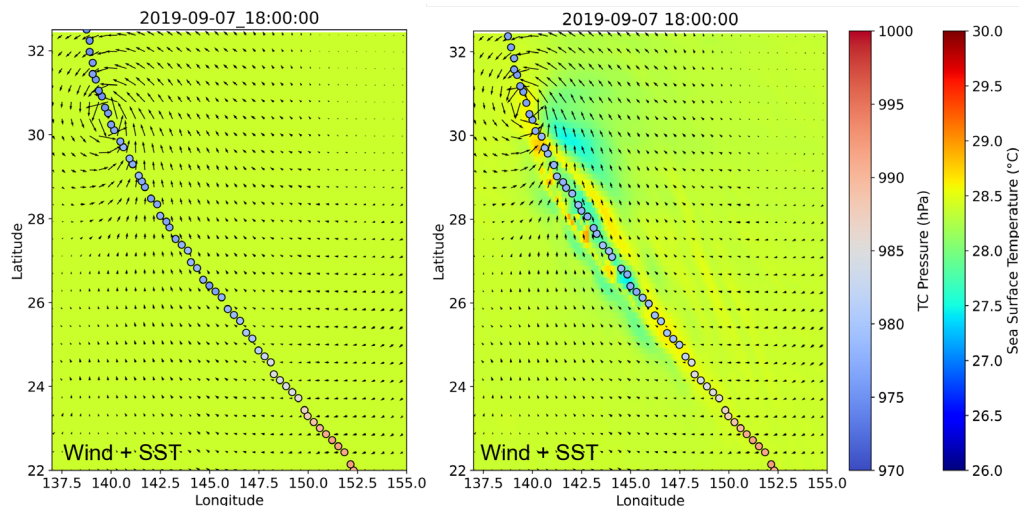


Figure 6. Snapshots of simulation results (left) the reference run (right) the coupled run.

Although the computational cost of these technologies remains high, leveraging the model's strong multiscale capabilities could lead to more refined and consistent predictions, spanning from offshore TC predictions to detailed coastal hazard assessments.

### Concluding Remarks

In this study, we extended the STOC model for use as an ocean model and developed the first prototype of a coupled model with the atmospheric model WRF. We demonstrated the applicability of STOC as an ocean model and discussed the results of the initial atmosphere-ocean coupled simulation tests. As discussed in the previous sections, the development of our coupled model is still in its early stages, and there are many aspects that require improvement and validation, such as computational stability, accuracy, and coupling issues. However, by extending STOC, originally specialized for coastal hazard assessment, to include the effects of TC-ocean interactions, the model holds potential to become a highly accurate and useful tool for TC and related disaster prediction (e.g., storm surges and coastal floodings), capturing the multiscale nature of coastal hazards from offshore to coastal regions. It is expected that further development will continue and that the potential for practical applications will be explored.

### REFERENCES

- Aiki, H., Yoshioka, M., Kato, M., Morimoto, A., Shinoda, T., and K. Tsuboki. 2015. A Coupled Atmosphere-Ocean-Surface-Wave Modeling System for Understanding Air-Sea Interactions under Tropical Cyclone Conditions. *Bulletin on Coastal Oceanography* 52(2): 139-148.
- Arikawa, T., Chida, Y., Seki, K., Takagawa, T., and K. Shimosako. 2019. Development and Applicability of Multiscale Multiphysics Integrated Simulator for Tsunami. *Journal of Disaster Research* 14(2): 225-234.
- Garcia, M., Choboter, P. F., Walter, R. K., and J. E. Castillo. 2019. Validation of the Nonhydrostatic General Curvilinear Coastal Ocean Model (GCCOM) for Stratified Flows. *Journal of Computational Science* 30: 143-156.
- Iida, K., Fudeyasu, H., Tanaka, Y., Iizuka, S., and Y. Miyamoto. 2023. Quantification and Attribution of Ocean Cooling Induced by the Passages of Typhoons Faxai (2019) and Hagibis (2019) Over the Same Region Using a High-Resolution Ocean Model and Cooling Parameters. *Atmospheric Science Letters* 24(9): e1169.
- Ito, K., Kuroda, T., Saito, K., and A. Wada. 2015. Forecasting a Large Number of Tropical Cyclone Intensities around Japan Using a High-Resolution Atmosphere-Ocean Coupled Model. *Weather and Forecasting* 30(3): 793-808.
- Jacob, S. D., and L. K. Shay. 2003. The Role of Oceanic Mesoscale Features on the Tropical Cyclone-Induced Mixed Layer Response: A Case Study. *Journal of Physical Oceanography* 33(4): 649-676.
- Landsea, C. W., and J. P. Cangialosi. 2018. Have We Reached the Limits of Predictability for Tropical Cyclone Track Forecasting? *Bulletin of the American Meteorological Society* 99(11): 2237-2243.
- Li, S., and C. Chen. 2022. Air-Sea Interaction Processes During Hurricane Sandy: Coupled WRF-FVCOM Model Simulations. *Progress in Oceanography* 206: 102855.
- Li, S., Chen, C., Wu, Z., Beardsley, R. C., and M. Li. 2020. Impacts of Oceanic Mixed Layer on Hurricanes: A Simulation Experiment With Hurricane Sandy. *Journal of Geophysical Research: Oceans* 125(11): e2019JC015851.
- Li, Z., Tam, C.-Y., Li, Y., Lau, N.-C., Chen, J., Chan, S. T., Huang, Y., et al. 2022. How Does Air-Sea Wave Interaction Affect Tropical Cyclone Intensity? An Atmosphere-Wave-Ocean Coupled Model Study Based on Super Typhoon Mangkhut (2018). *Earth and Space Science* 9(3): e2021EA002136.
- Marchesiello, P., Auclair, F., Debreu, L., McWilliams, J., Almar, R., Benshila, R., and F. Dumas. 2021. Tridimensional Nonhydrostatic Transient Rip Currents in a Wave-Resolving Model. *Ocean Modelling* 163: 101816.
- Price, J. F. 1981. Upper Ocean Response to a Hurricane. *Journal of Physical Oceanography* 11(2): 153-175.
- Shirai, T., Enomoto, Y., Watanabe, M., and T. Arikawa. 2022. Sensitivity Analysis of the Physics Options in the Weather Research and Forecasting Model for Typhoon Forecasting in Japan and Its Impacts on Storm Surge Simulations. *Coastal Engineering Journal* 64(4): 506-532.
- Skamarock, W., Klemp, J., Dudhia, J., Gill, D., Barker, D., Duda, M., Powers, J., et al. 2008. A Description of the Advanced Research WRF Version 3.

- Warner, J. C., Armstrong, B., He, R., and J. B. Zambon. 2010. Development of a Coupled Ocean–Atmosphere–Wave–Sediment Transport (COAWST) Modeling System. *Ocean Modelling* 35(3): 230-244.
- Yu, H., Chen, G., Zhou, C., Wong, W. K., Yang, M., Xu, Y., Hu, X., et al. 2022. Are We Reaching the Limit of Tropical Cyclone Track Predictability in the Western North Pacific? *Bulletin of the American Meteorological Society* 103(2): E410-E428.
- Zarzycki, C. M. 2016. Tropical Cyclone Intensity Errors Associated with Lack of Two-Way Ocean Coupling in High-Resolution Global Simulations. *Journal of Climate* 29(23): 8589-8610.
- Zhang, H., Chen, D., Zhou, L., Liu, X., Ding, T., and B. Zhou. 2016. Upper Ocean Response to Typhoon Kalmaegi (2014). *Journal of Geophysical Research: Oceans* 121(8): 6520-6535.
- Zhang, H., He, H., Zhang, W.-Z., and D. Tian. 2021. Upper Ocean Response to Tropical Cyclones: A Review. *Geoscience Letters* 8(1): 1.
- Zhang, Y., Meng, Z., Zhang, F., and Y. Weng. 2014. Predictability of Tropical Cyclone Intensity Evaluated Through 5-Year Forecasts with a Convection-Permitting Regional-Scale Model in the Atlantic Basin. *Weather and Forecasting* 29(4): 1003-1023.
- Zhao, X., and J. C. L. Chan. 2017. Changes in Tropical Cyclone Intensity with Translation Speed and Mixed-Layer Depth: Idealized WRF-ROMS Coupled Model Simulations. *Quarterly Journal of the Royal Meteorological Society* 143(702): 152-163.